

# Performance Modeling of a Piezohydraulic Actuator with Active Valves

H. Tan, W. Hurst, and D. J. Leo\*

Center for Intelligent Material Systems and Structures  
Mechanical Engineering Department Virginia Tech

## ABSTRACT

Piezohydraulic actuation is the use of hydraulic fluid to rectify the high frequency, small stroke oscillation movement of the piezoceramic stack into a unidirectional movement. This paper presents a quasi-steady incompressible flow model and a compressible flow model for performance simulation. These two models are derived based on the energy equations for hydraulic flow in circular pipe. Major losses and minor losses are identified and incorporated in the model. Assumptions and approximations were made to minimize computation effort while achieving good accuracy. A piezohydraulic actuation system with active valves is then built and tested. Comparison with test results shows that the simulations accurately predict system performance under loads at which value leakage is not present. The results reveal that friction losses due to viscosity are a major limitation of performance for the current test setup when operating at higher frequencies.

## 1. INTRODUCTION

Piezoelectric ceramics can produce large stress but are limited in their strain output. Conventional materials can produce blocked stresses on the order of 25-50 MPa at field levels of 1-2 MV/m, but the strain output is limited to 0.1% to 0.15%. Newer single-crystal ceramics produce larger strain levels ( 1%) but lower stresses ( 10-20 MPa) at equivalent field levels.

For the last two to three years several groups have studied piezohydraulic actuation as a means of overcoming the strain limitations in piezoelectric ceramics without sacrificing force capability. The first use of piezoelectric materials for producing 1-10 W mechanical power output was reported by Mauck and Lynch (1; 2). They discuss the development of a system consisting of a reciprocating piezoelectric pump and passive check valves. They report a no-load speed of 72.5 mm/sec and a blocked force of 271 N for a particular value of cylinder bore diameter (3). Assuming a linear relationship between these parameters, the maximum mechanical power output is estimated to be 5 Watts. More recently, Regelbrugge and Anderson numerically analyzed the performance of a piezohydraulic system and highlighted the need for systems-level analysis (4). Further experimental work was performed by Sirohi and Chopra (5). A maximum no-load velocity of 1.2in/sec. and block force of 35lbs was reported.

Our work in piezohydraulic actuation has focused on the development of systems that incorporate active valves for flow control. Our previous modeling efforts have concentrated on the development of lumped parameter models of piezohydraulic systems (6) and experimental demonstration of a closed hydraulic circuit (7; 8). Our experimental results demonstrate the importance of valve timing and fluid compressibility in the optimization of the output power of the system. These results qualitatively match our numerical analysis of the effects of compressibility on the efficiency of piezohydraulic and piezopneumatic systems (9).

In this work we present quasi-static steady flow models based on different approximations of the hydraulic fluid. In the first model, we assume a fully-developed incompressible viscous flow and in the second model we incorporate the compressibility of hydraulic fluid into our model. These two models are derived based on the energy equations for hydraulic flow in circular pipe. Major losses and minor losses are identified and incorporated in the model. Assumptions and approximations were made to minimize computation effort while achieving good accuracy. A prototype piezohydraulic system with active valves was then built and tested.

---

\*Further author information: (Send correspondence to Dr. Donald Leo), E-mail: donleo@vt.edu

# Report Documentation Page

Form Approved  
OMB No. 0704-0188

Public reporting burden for the collection of information is estimated to average 1 hour per response, including the time for reviewing instructions, searching existing data sources, gathering and maintaining the data needed, and completing and reviewing the collection of information. Send comments regarding this burden estimate or any other aspect of this collection of information, including suggestions for reducing this burden, to Washington Headquarters Services, Directorate for Information Operations and Reports, 1215 Jefferson Davis Highway, Suite 1204, Arlington VA 22202-4302. Respondents should be aware that notwithstanding any other provision of law, no person shall be subject to a penalty for failing to comply with a collection of information if it does not display a currently valid OMB control number.

1. REPORT DATE <b>00 JUN 2003</b>		2. REPORT TYPE <b>N/A</b>		3. DATES COVERED <b>-</b>	
4. TITLE AND SUBTITLE <b>Performance Modeling of a Piezohydraulic Actuator with Active Valves</b>				5a. CONTRACT NUMBER	
				5b. GRANT NUMBER	
				5c. PROGRAM ELEMENT NUMBER	
6. AUTHOR(S)				5d. PROJECT NUMBER	
				5e. TASK NUMBER	
				5f. WORK UNIT NUMBER	
7. PERFORMING ORGANIZATION NAME(S) AND ADDRESS(ES) <b>Center for Intelligent Material Systems and Structures Mechanical Engineering Department Virginia Tech</b>				8. PERFORMING ORGANIZATION REPORT NUMBER	
9. SPONSORING/MONITORING AGENCY NAME(S) AND ADDRESS(ES)				10. SPONSOR/MONITOR'S ACRONYM(S)	
				11. SPONSOR/MONITOR'S REPORT NUMBER(S)	
12. DISTRIBUTION/AVAILABILITY STATEMENT <b>Approved for public release, distribution unlimited</b>					
13. SUPPLEMENTARY NOTES <b>See also ADM001697, ARO-44924.1-EG-CF, International Conference on Intelligent Materials (5th) (Smart Systems &amp; Nanotechnology)., The original document contains color images.</b>					
14. ABSTRACT					
15. SUBJECT TERMS					
16. SECURITY CLASSIFICATION OF:			17. LIMITATION OF ABSTRACT <b>UU</b>	18. NUMBER OF PAGES <b>8</b>	19a. NAME OF RESPONSIBLE PERSON
a. REPORT <b>unclassified</b>	b. ABSTRACT <b>unclassified</b>	c. THIS PAGE <b>unclassified</b>			

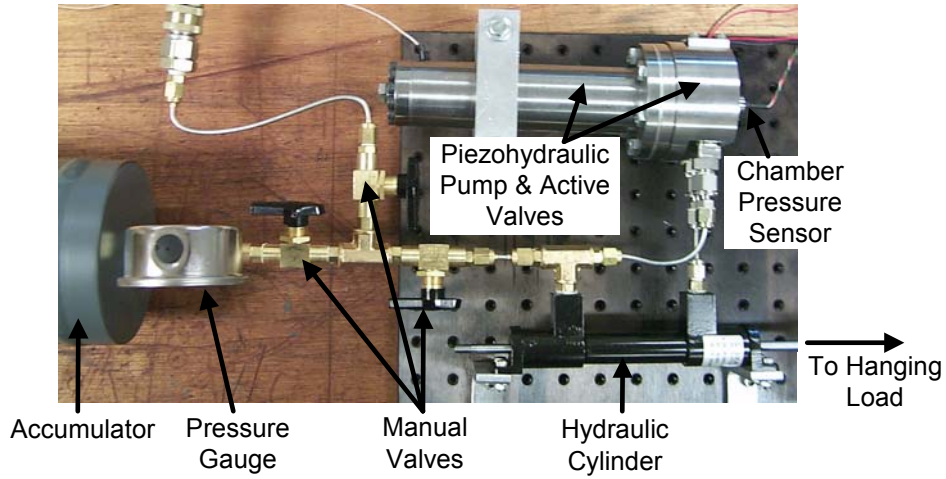


**Figure 1:** Bench Top Experimental Test Setup

**Table 1:** Status of stack and valves at four stages.

	Compression	Exhaustion	Expansion	Intake
Stack	expanding	expanding	retracting	retracting
Inlet	closed	closed	closed	open
Outlet	closed	open	closed	closed

## 2. SYSTEM MODELS

A typical piezohydraulic pump consists of five major components: a stack actuator, a pumping chamber, an accumulator, a hydraulic cylinder and valves and fittings. Figure 1 shows the prototype of the piezohydraulic pump. The active valves are used to control the flow of the hydraulic fluid. An accumulator is used to provide the system with a bias pressure.

The model of the system will be introduced based on the four stage operation fashion (9). The stack actuator moves in a reciprocal fashion under periodic electrical excitation. The operation of the system can be divided into four stages: compression, exhaustion, expansion and intake based on the phases of valve operation related to the stack. Table 1 shows the status of valves and stack in each stage. For this four stage model, it is noticed that only in exhaustion stage does the system perform work on the load.

Laminar flows and turbulent flows are very different flow patterns which are determined by the Reynolds's number of the flow. For flow in pipes, it is laminar when Reynolds's number is less than 2000 and flow is usually turbulent when it is larger than 3000. The critical operation frequency for laminar flow was determined in (10) to be  $f_{cr} = 960$  Hz. For operation frequency below 960 Hz, the flow can be considered as laminar.

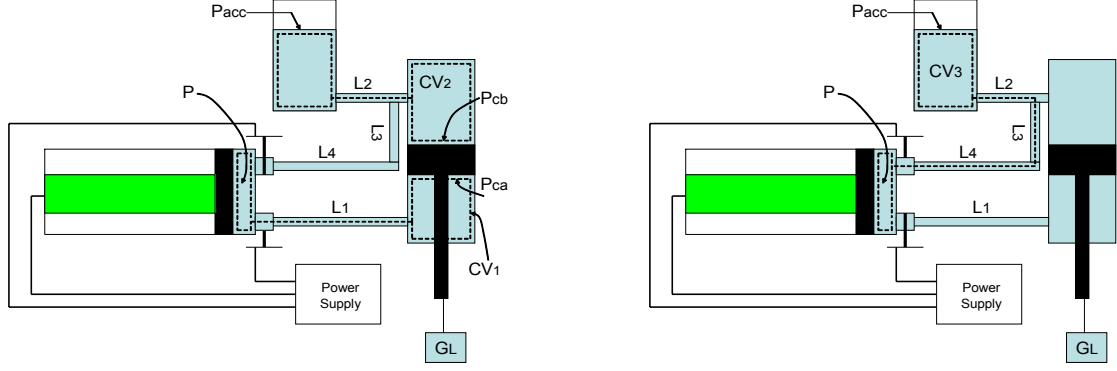
### 2.1. Incompressible viscous flow (IVF) model

When developing this flow model, we assume an incompressible flow in the open chamber operations: the *exhaustion* stage and *intake* stage, while the compressibility is considered in the closed chamber operations: the *compression* stage and *expansion* stage.

The electromechanical coupling model of the piezoceramic stack will be incorporated into the flow equations, which enable us to simulate response under a certain characteristics of a power output. Nasser and Leo (9) presented a one dimensional model for piezoceramic stack with many layers of piezoelectric elements:

$$x = x_0 V - \frac{1}{K_a} F, \quad (1)$$

$$Q = CV - x_0 F. \quad (2)$$



(a) Control volumes in the exhaustion stage

(b) Control volumes in the intake stage

**Figure 2:** Control volumes for IVF model

where  $x$  is the displacement of stack,  $V$  denotes the voltage applied to the stack,  $Q$  represents the charge and  $F$  is the force generated by the stack, which is equal to the pressure times with cross section area of chamber  $A_{ch}$ . The variable  $x_0$  denotes the displacement-to-voltage constant of the stack,  $K_a$  is the stiffness and  $C$  is stress-free capacitance of the piezoceramic stack. This coupling model will be incorporated into the flow model which will be developed in the following sections.

At beginning of a cycle, we assume that the system is pre-pressurized to  $P_1$ , the initial volume in the pumping chamber is  $\forall_0$  and the displacement of the piston is  $x_1$ . Then the system begins to operate in the four stage fashion. The models developed for each stage can be integrated to simulate the full cycle operation of the system.

### Compression Stage

In this analysis, we assume that the bulk modulus of the fluid  $\beta$  is a constant, which is defined by

$$\beta = -\frac{dP}{d\forall/\forall}. \quad (3)$$

Integrating the above equation and substituting in the initial conditions yields

$$P = P_1 - \beta \ln \frac{\frac{\forall_0}{A_{ch}} - x}{\frac{\forall_0}{A_{ch}} - x_1}, \quad (4)$$

### Exhaustion Stage

We assume the initial states of the stage is  $x = x_2$  and  $P = P_2$ . In this stage, the fluid flows from the pumping chamber into the high side of the cylinder. And the piston in the cylinder pushes the fluid to flow into the accumulator.

The energy equation of fully-developed steady laminar flow in a pipe is derived by White (11)

$$\left(\alpha_1 \frac{\bar{V}_1^2}{2} + \frac{p_1}{\rho}\right) - \left(\alpha_2 \frac{\bar{V}_2^2}{2} + \frac{p_2}{\rho}\right) = h_l, \quad (5)$$

where subscript 1 and 2 denotes the physical variables at different sections of the pipe. For a laminar flow the coefficients of velocity profile is a constant:  $\alpha_1 = \alpha_2 = 2$ . To apply the above energy equation, control volumes are chosen as the dash lines in Figure 2(a).

To simplify the computation, following geometry constants are defined.  $\lambda$  is defined as the area of chamber to the piping and  $\gamma$  is defined as area ratio of the hydraulic cylinder. For a single-ended cylinder  $\gamma$  is larger than 1 and for a double-ended one it is equal to 1. The variable  $\epsilon$  is defined as the area ratio of the hydraulic cylinder to the pipe. Substitute the above constants into Equation (5) and simplify to yield

$$P - P_{ca} = \left(\frac{\epsilon^2 K_{L1}}{2} + \lambda^2 - 1\right) \rho \dot{x}^2. \quad (6)$$

In the same manner, we can derive the flow equations for the control volume  $CV_2$  by determine the major losses and minor losses through the control volume as shown in Figure 2(a). The energy equation for control volume  $CV_2$  is

$$P_{cb} - P_{acc} = \left( \frac{\gamma^2 \epsilon^2}{2\lambda^2} K_{L2} - 1 \right) \cdot \rho V_L^2, \quad (7)$$

where  $P_{cb}$  is low side pressure and  $P_{acc}$  is accumulator pressure. Simplifying Equation (6), (7) and substituting the constitutive equation of stack yields

$$\begin{aligned} \dot{P} &= -\frac{K_a}{A_{ch}} \sqrt{\frac{1}{\Omega \rho} \left( P - \gamma \left( P_{acc} + \frac{G_L}{A_{cy}} \right) \right)} + \frac{x_0 K_a}{C A_{ch}} i \\ \Omega &= \left( \frac{\epsilon^2}{2} (K_{L1} + \gamma^3 K_{L2}) - (\gamma - 1) \lambda^2 - 1 \right). \end{aligned} \quad (8)$$

Equation (8) is a non-linear first order differential equation. For a current controlled stack, the input current  $i$  of the stack depends on the characteristic of the power supply. We can solve the differential equation of the pressure in Equation (8) if the dynamics of the input current are known.

### Expansion Stage

Assuming the initial pressure is  $P_3$  and initial displacement  $x_3$ , the equation of expansion stage becomes

$$P = P_3 - \beta \ln \frac{\frac{V_0}{A_{ch}} - x}{\frac{V_0}{A_{ch}} - x_3}. \quad (9)$$

### Intake Stage

This stage is similar to the exhaustion stage. Figure 2(b) shows the control volume  $CV_3$  in dashed lines. Using the same procedure as in the exhaustion stage, the flow equations in the intake stage are

$$\dot{P} = \frac{K_a}{A_{ch}} \sqrt{\frac{1}{\Theta \rho} (P_{acc} - P)} + \frac{x_0 K_a}{C A_{ch}} i, \quad (10)$$

where  $\Theta = \left( \frac{\epsilon^2 K_{L3}}{2} + 1 \right)$  and  $K_{L3}$  is the loss coefficient in the control volume.

In the above paragraph, the equations of flow in each stage are derived respectively. Thus, the operations of the system in one full 4-stage cycle can be modeled by combining these equations.

#### 2.1.1. Summary of IVF model

In the IVF model, we assume a viscous incompressible flow. The viscosity is taken into account in order to predict energy loss in the hydraulic components. Reynolds number is computed to determine the flow in the system. The flow equations in each stage is derived based on the energy equations. By assuming the fluid is incompressible, the IVF model is described by only one first order differential equation and is easy to solve but it might overestimate the performance by ignoring the compressibility of the fluid.

#### 2.2. Compressible viscous flow (CVF) model

In this model, compressibility of the fluid will be modeled in the full cycle of the four stages. Because we already assumed compressibility in the *compression* stage and *expansion* stage in the development of the IVF model, equations of motion of IVF model in these two stages are the same for CVF model. Thus, we only need to derive the flow equations for the *exhaustion* stage and *intake* stage.

The system is considered as seven components of fluid as shown in Figure 3. To maintain the simplicity of the model, assumptions and approximations are made based on observation of the setup. First assumption is that we assume energy losses, including major losses and minor losses only exist in the pipes, fittings and valves. we assume compressibility of fluid only occurs in pumping chamber and high side of the cylinder, which corresponds to part 1 and 3 respectively in Figure 3. We neglect the compressibility in component 4. The reason is that it is directly connected with the accumulator, which means the pressure variation is small and thus we can consider the density is constant. Because the cross section area of pipe is very small and the length of pipe in part 2 is made short as possible to reduce energy losses, we can assume the fluid volume in the pipe is relatively small

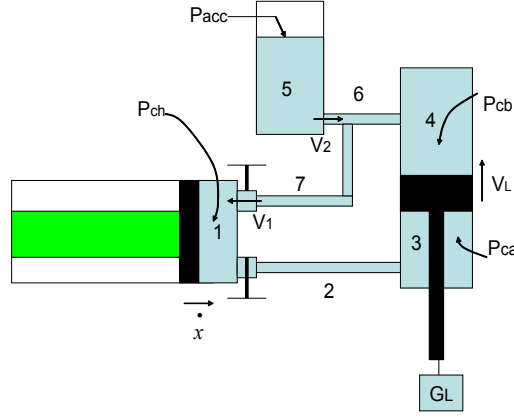


**Figure 3:** Diagram of system used to develop CVF model.

	<i>Components**</i>	IVF MODEL	CVF MODEL
Compression	1	$P_{ch} = \beta \frac{A_{ch}}{\sqrt{-A_{ch}x}} \dot{x}$	SAME
Exhaustion	1	$\dot{\rho} = 0$	$\dot{\rho}_{ch} = \rho_{ch} \frac{-V_1 A_p + x A_{ch}}{L_0 - x}$
	2	$V_1^2 + \frac{P_{ch}}{\rho_{ch}} = V_L^2 + \frac{P_{ca}}{\rho_{ca}} + K_{L1} \frac{V_2^2}{2}$	SAME
	3	$\dot{\rho} = 0$	$\dot{\rho}_{ca} = \rho_{ca} \frac{V_2 \frac{x}{L_0} + V_L}{L_0 - x}$
	4,5,6	$P_{cb} = P_{acc} + K_{L2} \rho_0 V_L^2 \frac{\epsilon^2 \gamma^2}{\lambda^2}$	SAME
Expansion	1	$P_{ch} = \beta \frac{A_{ch}}{\sqrt{-A_{ch}x}} \dot{x}$	SAME
Intake	1	$\dot{\rho} = 0$	$\dot{\rho}_{ch} = \rho_{ch} \frac{V_1 \lambda + \dot{x}}{L_0 - x}$
	5,6,7	$V_2^2 + \frac{P_{acc}}{\rho_0} + K_{L3} \frac{V_2^2}{2} = V_1^2 + \frac{P_{ch}}{\rho_{ch}}$	SAME

\*\* Refer to Figure 3

**Table 2:** Key equations of IVF and CVF model at each stage.

compared to the volume in the pumping chamber and hydraulic cylinder. Thus we neglect the mass changes of fluid in pipes of component 2.

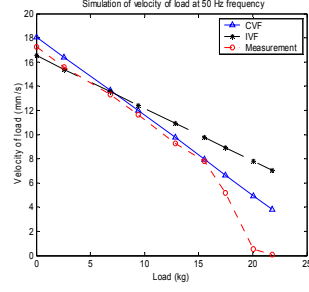
The density of fluid is no longer a constant as in the incompressible model. The density-pressure relationship of fluid can be derived from the definition of bulk modulus in Equation (3) as following

$$\frac{d\rho}{\rho} = \frac{1}{\beta} dP. \quad (11)$$

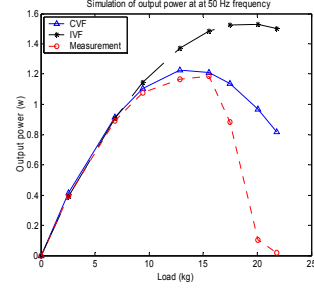
The approach of this modeling is to incorporate the density variation into the incompressible model. The key equations of the hydraulic components in each stage are summarized in the Table 2. The second column is the component corresponding to Figure 3. The energy equations of CVF model is the same as IVF model. The only difference is the continuity equation in the pumping chamber and hydraulic cylinder, where density change is taken into account. The CVF model involves coupled differential equations and can be numerically solved.

### 3. EXPERIMENTAL SETUP

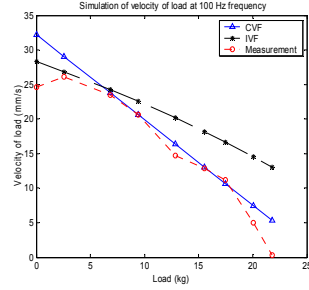
The bench top experimental setup used can be seen in Figure 1. The experimental setup incorporated active valves comprised of a small piezoceramic stack to pump fluid and move a hydraulic cylinder. Using the setup as seen in Figure 1, experiments were conducted to characterize the overall actuator performance. The piezoceramic stack actuator and active valves were all driven and controlled by a dSPACE system that also acquired and recorded the data from the sensors used in the experiments. A Sentec pressure sensor is used to measure the pressure inside the chamber. A Polytec GmbH laser vibrometer (model OFV 303) and controller (model OFV 3001) were used to measure the motion of a target connected to the end of the hydraulic cylinder. The laser vibrometer measured the cylinder displacement over a finite amount of time while pulling the load.



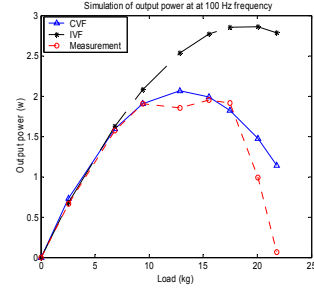
(a) Velocity comparison at 50 Hz



(b) Power comparison at 50 Hz



(c) Velocity comparison at 100 Hz



(d) Power comparison at 100 Hz

**Figure 4:** Comparison of simulated and experimental velocity and power for a single-ended cylinder.

## 4. COMPARISON OF SIMULATIONS AND TEST RESULTS

### 4.1. Simulation parameters

The model of IVF and CVF presented derived in the previous section will be used to predict the performance and efficiency calculations. In the simulations performed in this paper the following parameters will be used:

- The bulk modulus of the fluid will be modeled as linear function of pre-pressure (10):

$$\beta = 48.8P + 15356, \quad \beta_0 = 15356, \quad \gamma = 48.8 \quad (12)$$

This linear model is characterized by closed chamber tests where stiffness of the fluid is measured.

- The density of fluid is assumed to be  $\rho = 900(kg/m^3)$ , which is a typical density for mineral oil. The viscosity  $\nu = 3 \times 10^{-5}(m/s^2)$ .

- Two setups were tested. The first one is the single-ended cylinder setup powered by DSM 2 Level PZT drive whole maximum current is 4.2 A. The other is the double-ended cylinder powered by DSM 3-channel power supply whose maximum current is 32.5 A.

### 4.2. Single-ended cylinder setup

The fluid was pre-pressured at 230 Psi for the first set of tests. Because the maximum operation frequency of the DSM 2 amplifier is 100 Hz, the system was tested at frequencies from 20 Hz up to 100 Hz. Through these tests, a timing scheme of 50% stack duty cycle and 40% valve duty cycle with 5% outlet valve offset and 55% inlet valve offset is adopted. The pressure in the pumping chamber, the displacement of load and displacement of the piston are measured.

Figure 4 shows the comparison of simulation results and experimental data for 50Hz and 100 Hz respectively. The CVF model is much more close to experimental data than IVF model in terms of both velocity and power. For loads up to 15 Kg, the simulation results of CVF model consist with the experimental data pretty well. It is noted the simulation velocity of both model are very like a straight line. But the slope of the CVF model is steeper than the slope of IVF. Accordingly, the difference of the two models becomes more obvious when the

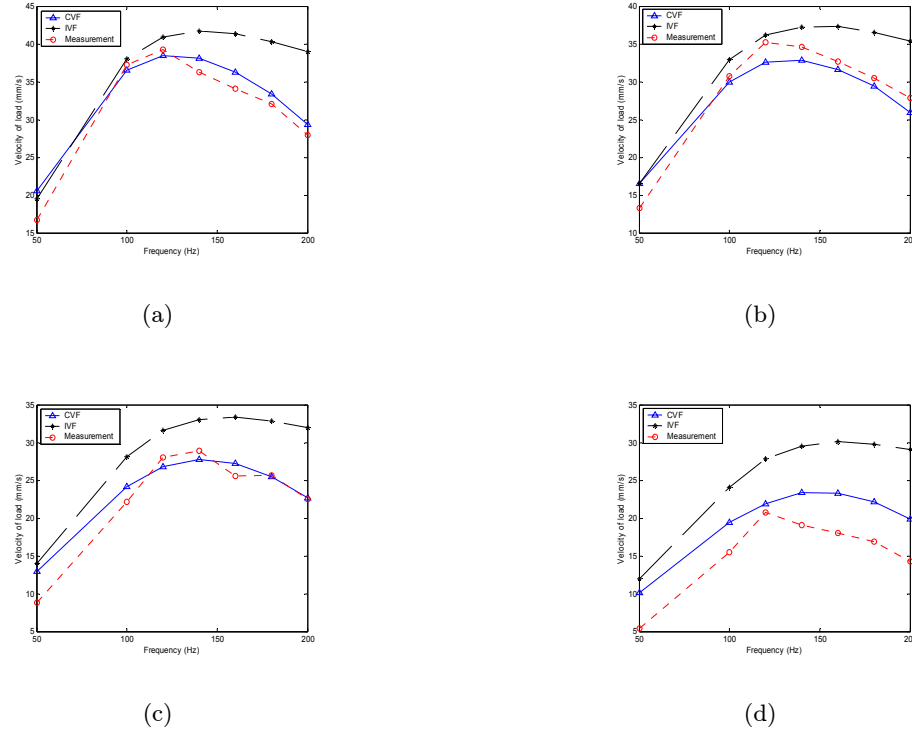


**Figure 5.** Comparison of simulated and experimental output power and velocity under 130 V stack excitation for a double-ended cylinder. (a),(b),(c),(d): Velocity at 0, 6.84, 12.82, 17.45 Kg.

load is larger than 7 Kg. The reason can be explained by the compressibility of the fluid. When a larger load is attached to the cylinder, the back pressure is increased, which reduces the stroke of the piezoelectric actuator. Thus the displacement of the load also decreases accordingly. Furthermore, due to the compressibility of the load, additional decrease of load displacement is inevitable. When the high pressure fluid in the chamber flows into the low pressure cylinder, the volume will increase due to pressure drop. A heavy load results in higher pressure in the cylinder and thus lower pressure drop, the effect of the volume increase by the pressure drop is reduced. This additional decrease of load displacement is not taken into account for the IVF models because they assume an incompressible fluid. Hence, the simulation results of IVF model overestimates system performance under large loads. It is also noted that for load heavier than 15Kg, the difference between the CVF model and experimental data increases. As the load increases over 15Kg, the measured velocity decreases very fast for both frequencies. We believe this fast drop of performance for heavy load is because the leakage problem of the valves.

### 4.3. Double-ended cylinder setup

The double-ended cylinder test bench was built in order to achieve better performance and it was tested using a new amplifier that enables operation in the kilo-hertz range. Different loads were attached with the output cylinder when operated in a series of frequencies.

The simulation of velocity versus frequency at different loads are plotted in the following figures. Due to the hydraulic amplification mechanism of the active valves, we expect some delay might be introduced. In the simulations, a 0.4 ms valve transition is assumed. Figure 5 compares respectively the velocities and power respectively the velocities of the IVF and CVF models with experimental results at 130 V peak voltages. The CVF model consists with the experimental model better than IVF model. The performance of the system topped at about 140 Hz. Once again, we notice that under heavy load, the large difference exists between the model simulation and experimental results. We also attribute this discrepancy to the leakage problem that is not accounted in the model simulations.

We observed that as the load increases the IVF model overestimates the system performance as it does in the single-ended cylinder setup, which can also be attributed to compressibility of fluid. Another observation is that the difference between the IVF and CVF becomes more obvious as frequency increases in each plot. The

reason of this discrepancy is that CVF model assumes a linear bulk modulus to pressure model while the IVF model assumes an infinite modulus. As the frequency goes higher, because the fluid can not flow fast enough to fill the chamber to the pre-pressure, the stiffness of the fluid decreased due to reduce of bulk modulus. A lower stiffness of fluid results in lower dynamic pressure and smaller stroke of the load in one cycle. This effect ends up to a big difference between the IVF model and CVF model when the pump is operated at frequency near 200 Hz. It indicates the compressibility of fluid is important to the performance of the system.

## 5. SUMMARY AND CONCLUSIONS

Two steady flow models are presented in this paper based on different approximation of the fluid. The incompressible viscous flow (IVF) model is developed in favor of minimizing computation effort by ignoring the compressibility of the hydraulic fluid. The compressible viscous flow (CVF) model is then presented in order to achieve more accurate results. While compressibility of fluid is taken into account, assumptions and approximations are carefully made to maintain the simplicity for numerical simulations.

A single-ended cylinder setup and a double-ended cylinder setup were developed and tested. The test results were compared with theoretical simulations. The comparison revealed the IVF model deviated from the CVF model under higher loads, which indicates the compressibility of the fluid is important for the performance of the stack. Increasing pre-pressure thus increasing bulk modulus of fluid can potentially improve the performance. Under low loads, it is accurate to use IVF model to predict performance. The CVF model provide better results under higher loads and the CVF model consists with test results well for loads up to 20Kg. But when the load is increased above that limit, the performance of the system drops more sharply than the model predicts. Combined with the reverse movement of load observed under large loads and the pressure drop in closed chamber figuration, we pretty confidently attribute the reason to the leakage problem through the valves.

The simulation results and experimental tests indicate that friction in the hydraulic circuits is a major limitation of the system performance when going to higher frequencies. The maximum stroke of piston decreases and peak pressure drops, resulting in a reduction of performance. The system performance is maximized when operated at around 140 Hz. Based on this observation, a possible effective way to optimize the system is to reduce friction and head losses in the hydraulic circuits.

## References

- [1] L. Mauck and C. S. Lynch, "Piezoelectric hydraulic pump," in *Proceedings of the SPIE*, **3668**, pp. 844–852, 1999.
- [2] L. Mauck and C. S. Lynch, "Piezoelectric hydraulic pump development," in *Proceedings of the SPIE*, (Paper Number 3985–85), 2000.
- [3] L. Mauck and C. S. Lynch, "Piezoelectric hydraulic pump development," *Journal of Intelligent Material Systems and Structures* **11**(10), pp. 758–764, 2000.
- [4] M. Regelbrugge and E. H. Anderson, "Solid-fluid hybrid actuation: Concepts, models, capabilities, and limitations," in *Proceedings of the Twelfth International Conference on Adaptive Structures Technology*, 2001.
- [5] J. Sirohi and I. Chopra, "Development of a compact piezoelectric-hydraulic hybrid actuator," in *Proceedings of the SPIE*, **4327**, pp. 401–412, 2001.
- [6] K. Nasser, D. J. Leo, and H. H. Cudney, "Compact piezohydraulic actuation system," in *Proceedings of the SPIE*, (Paper Number 3991-41), 2000.
- [7] K. Nasser, N. Vujic, D. Leo, and H. Cudney, "Modeling and testing of a piezohydraulic actuation system," in *Proceedings of the SPIE*, **4327**, pp. 354–365, 2001.
- [8] K. M. Nasser, "Development and analysis of the lumped parameter model of a piezohydraulic actuator," Master's thesis, Virginia Polytechnic Institute and State University, 2000.
- [9] K. M. Nasser and D. J. Leo, "Efficiency of frequency-rectified piezohydraulic and piezopneumatic actuation," *Journal of Intelligent Material Systems and Structures* **11**(10), pp. 798–810, 2000.
- [10] H. Tan, "Performance modeling and efficiency analysis for a piezohydraulic pump with active valves," Master's thesis, Virginia Polytechnic Institute and State University, 2002.
- [11] F. M. White, *Fluid Mechanics*, Third Edition, McGRAW-HILL, Inc., 1994.